

## Inverse multiple scattering in the downward-continuation approach

Alison E. Malcolm\*, Maarten V. de Hoop  
Center for Wave Phenomena, Colorado School of Mines

### Summary

Internal multiples have long been recognized as a problem in seismic imaging. Some theoretical developments have been made to attenuate them, but there is no 3D theory as yet that is valid for a wide range of velocity models. The goal of this paper is to present such a theory. Through the development of this theory we show that, unless certain simplifying assumptions are made about the velocity model, estimating multiples is velocity-model-dependent. We propose estimating and subtracting the multiples in the image domain rather than the data domain. In common-image gathers, the redundancy of well-corrected primaries can be exploited to improve adaptive subtraction techniques.

### Introduction

There are two distinct methods used to attenuate multiples. The first is a signal processing approach in which differences in moveout between primaries and multiples are exploited to filter out multiples. The second is a wave-theoretic approach in which the multiples are modeled and then subtracted from the data. We present an approach in the second category to attenuate internal multiples.

Our approach is similar to that of Weglein *et al.* [8] and ten Kroode [7], in that we express the multiples in terms of the data through a series representation of the wavefield in terms of the medium contrast. Our approach is different in that we use a hybrid between the Lippmann-Schwinger and Bremmer series instead of the Lippmann-Schwinger series alone. The advantage of this approach is that the Bremmer series allows the separation of the wavefield into its up- and down-going constituents. This allows the natural application of the restriction applied by ten Kroode to ensure that the central scatter is shallower than the two other scatters (i.e.,  $z_1 > z_2$  and  $z_1 > z_3$  in Fig. 2). Additionally, de Hoop [1] gives convergence estimates on the Bremmer series, which do not exist for the Lippmann-Schwinger series.

Our approach goes beyond the work of Weglein *et al.* [8], and ten Kroode [7] in that where they considered one- and two-dimensional media without caustics, our approach is applicable in three dimensions in the presence of caustics. Ten Kroode found that the Weglein *et al.* method of attenuating multiples is independent of the velocity model only if the traveltime increases monotonically with depth as illustrated in Fig. 1. In moving beyond this assumption we find that modeling multiples does require information about the medium.

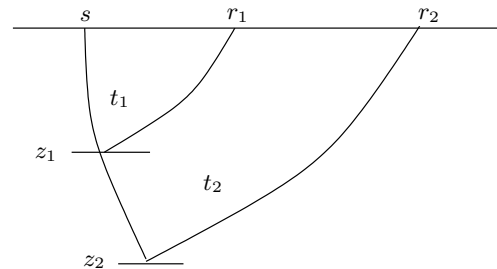


Fig. 1: Illustration of the traveltime monotonicity assumption. The assumption states that  $t_1 < t_2$  if  $z_1 < z_2$ , where  $t_1$  is the time along the ray-path from  $s$  to  $r_1$  and  $t_2$  is the time along the ray-path from  $s$  to  $r_2$ . This figure is modeled after ten Kroode's [7] Fig. 8.

We propose subtracting the multiples in the image domain rather than the data domain. It is easier to subtract the multiples in the image domain because correctly imaged primaries are flat in common image gathers (CIGs). Thus it is easier to differentiate between primaries and multiples in this domain. Ways to exploit this in a signal-processing framework are discussed by Sava and Guitton [4]. This redundancy will also allow more freedom in the adaptive subtraction phase of multiple attenuation. Adaptive subtraction compensates for differences in illumination between multiples and primaries as well as amplitude errors in multiple estimation.

### Inverse Lippmann-Schwinger-Bremmer Series

We derive both a forward (image  $\mapsto$  data) and an inverse (data  $\mapsto$  image) series representation using a hybrid between the Lippmann-Schwinger and Bremmer series approaches. The hybrid series uses the directional decomposition of the Bremmer series, along with the Lippmann-Schwinger medium decomposition into a known, smooth reference and unknown, singular perturbation. This allows us to trace waves through their up and down scatters while still preserving the contrast source formulation of the Lippmann-Schwinger construction. From the third term of the forward series, we model the triply scattered data and from the third term of the inverse series we estimate the third-order (in the data) contribution to the image.

The expression for the first and third terms in the inverse series is

$$V_1 + V_3 = M(d - \mathcal{L}(V_1 \mathcal{L}(V_1 \mathcal{L}(V_1 U_0))), \quad (1)$$

where  $V = \sum V_j$  is the medium contrast,  $M$  is an imaging/migration operator, and  $d$  is the recorded data. The

## Inverse multiple scattering

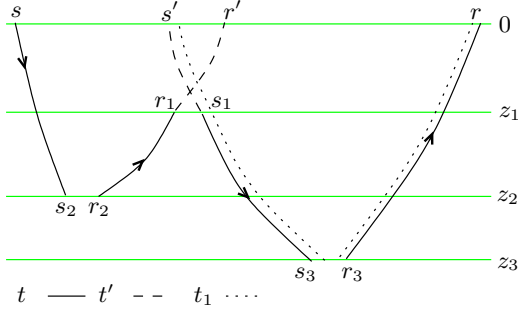


Fig. 2: Triple scattering notations and conventions. The quantity  $s_j$  is the source location at the  $z_j$  depth level, and  $r_j$  is the receiver location at  $z_j$ . In this figure, the imaging condition has been not applied at each depth level, thus  $s_j$  and  $r_j$  are not equal.

quantity  $V_1 = M(d)$  is the first-order approximation to the medium contrast,

$$\mathbf{L} = \begin{pmatrix} G_+ & 0 \\ 0 & G_- \end{pmatrix},$$

is the matrix of up- and down-going Green functions ( $G_+$  and  $G_-$  are the up- and down-going Green functions respectively) and  $U_0$  is the wavefield in the background model. The structure of (1) is like that of Lippmann-Schwinger; however the operators  $\mathbf{L}$ ,  $V_1$ ,  $V_3$  and  $M$  come from the Bremmer series rather than from Lippmann-Schwinger. As is the case in the standard Lippmann-Schwinger formulation, we use that  $\mathbf{L}(V_1\mathbf{L}(V_1U_0)) = \mathbf{L}(V_3U_0)$ , where  $V_3$  is the third order, in the data, contribution to the medium contrast.

### Internal Multiples

To make use of the formalism introduced in (1), we need to construct two images, one from the data  $d$  and the other from an estimate of the triply scattered data  $d_3 = \mathbf{L}(V_3U_0)$ . The  $d_3$  data set is not directly available, and so must be estimated from the available data. We use the downward-continuation approach to carry out this step.

To model the internal multiple data set  $d_3$ , we first require a method of modeling primaries. Using the downward-continuation approach, we model singly scattered data, following Stolk and de Hoop [5], via

$$d_1(s, r, t) = \frac{1}{4} D_t^2 Q_r^*(0) Q_s^*(0) \int_0^\infty dz_1 H(0, z_1) Q_{r_1}(z_1) Q_{s_1}(z_1) (E_1 E_2 a)(z_1, s_1, r_1, t_1), \quad (2)$$

where  $d_1$  is the singly scattered data, at source  $s$ , receiver  $r$ , and time  $t$  and  $D_t = i\partial_t$ . We denote by  $H(0, z_1)$  the flux-normalized propagator of the double-square-root equation, which propagates the wavefield from the depth  $z_1$  to 0. The  $Q$  operators diagonalize the wave equation, written as a first-order system [5]; \* denotes an operator

adjoint. These operators influence the amplitudes but not the traveltimes of arriving waves. The medium contrast  $a = \delta c/c_0^3$  is mapped to data at time zero, with coincident source and receiver positions, through the  $E_1$  and  $E_2$  operators. These operators apply the adjoint of the imaging condition, mapping the image to data at time zero, with coincident source and receiver positions. The notation is illustrated in Fig. 2.

From these modeled data, we construct two other pseudo-data-sets that model some portion of the wavefield. First we have

$$d'_1(z_1, s, r, t) = D_t^2 Q_s^*(0) Q_r^*(0) H(0, z_1) Q_{s_1}(z_1) Q_{r_1}(z_1) (E_1 E_2 a)(z_1, s_1, r_1, t_1), \quad (3)$$

which are data generated by a particular layer,  $z_1$ , in the subsurface. Second, we construct

$$\mathbf{d}_1(z_1; s, r, t) = \int_{z_1}^\infty dz d'_1(z, s, r, t) \quad (4)$$

$$= d_1(s, r, t) - \int_0^{z_1} dz d'_1(z, s, r, t), \quad (5)$$

which is data scattered strictly below the depth  $z_1$ . We also have the relation

$$H(z_1, 0) d_1(s, r, t) = H(z_1, 0) \mathbf{d}_1(z_1; s, r, t), \quad (6)$$

i.e., after downward continuing the data to the depth  $z_1$ ,  $d_1$  and  $\mathbf{d}_1$  are the same.

With the above definitions, we can model internal multiples via

$$d_3(s, r, t) = \int_0^\infty dz_1 \int ds' \int dr' \int_{\mathbb{R}_+} dt' Q_{s'}^*(0)^{-1} Q_{r'}^*(0)^{-1} d'_1(z_1, s', r', t') Q_{s'}^*(0)^{-1} Q_{r'}^*(0)^{-1} \int_{\mathbb{R}_+} dt_1 \mathbf{d}_1(z_1; s', r, t + t' - t_1) \mathbf{d}_1(z_1; s, r', t_1); \quad (7)$$

the different time variables pertain to the paths illustrated in Fig. 2;  $s'$  and  $r'$  are the surface positions of the data continued from the central scattering point to the surface, also illustrated in Fig. 2. This is just one of several equivalent methods of estimating  $d_3$ . In whichever way it is modeled,  $d_3$  has errors of order higher than 3. These errors could be corrected by computing  $d_5$ , which models contributions from second-order internal multiples, resulting in errors of order higher than 5.

To construct both  $\mathbf{d}_1$  and  $d'_1$ , knowledge of the velocity model is required down to the depth  $z_1$ . This knowledge is required to either model data from this depth to construct  $d'_1$  and  $\mathbf{d}_1$  through (5), or to downward continue the data  $d_1$  to the depth  $z_1$  as in (6). If the traveltime monotonicity assumption of ten Kroode [7] is satisfied, this modeling can be replaced by a time-windowing procedure applied to the data. The condition results from the requirement that the  $z_2$  and  $z_3$  depth levels are deeper than the  $z_1$

## Inverse multiple scattering

level. Ten Kroode's traveltime monotonicity assumption allows this condition on the depth to be replaced by a relation between the traveltimes of the three data sets. In this case,  $\mathbf{d}_1$  becomes independent of  $z_1$ , and the  $z_1$  integral can be combined with  $d'_1$ , giving  $d_1$ .

### Inverse Scattering

Subtracting multiples in the data domain is difficult for a number of reasons. For example, in the data domain events coming from different regions of the subsurface are difficult to separate. Thus, removing multiples becomes more challenging since the multiple energy is mixed with several different events. In contrast, correctly imaged primaries appear flat in CIGs. Multiples, since they are not imaged correctly, will show residual moveout in CIGs. We propose a wave-theoretic approach to estimate the contribution of multiples in the image domain.

From the series representation given in (1), we find that the contribution to the image made by multiples can be computed by applying the single-scattering migration operator to the triply scattered data. Replacing the operator  $M$  in (1) with either the wave-equation migration operator,  $M_{WE}$ , or the wave-equation angle transform,  $A_{WE}$ , [6] we find the first- and third-order contributions to the image via

$$\langle a_1 \rangle(x, z) = M_{WE}d \quad (8)$$

$$\langle a_3 \rangle(x, z) = M_{WE}\langle d_3 \rangle \quad (9)$$

$$\langle\langle a_1 \rangle\rangle(x, z, p) = A_{WE}d \quad (10)$$

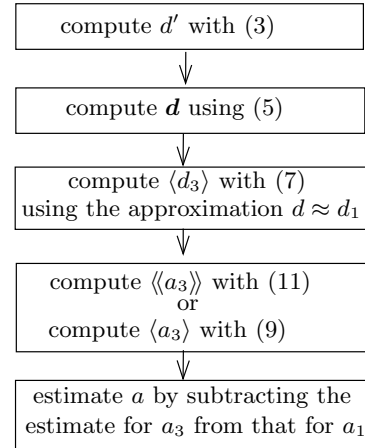
$$\langle\langle a_3 \rangle\rangle(x, z, p) = A_{WE}\langle d_3 \rangle, \quad (11)$$

where  $p$  is the slowness,  $a_1$  is the first-order estimate of the image and  $a_3$  the third order estimate. (The medium contrast  $V$  in (1) is a function of both  $a$  and the  $Q$  operators introduced in the previous section.) The angle brackets denote that these quantities are estimates. To obtain a final image, we need to combine the first- and third-order estimates. The series construction (1) shows that this is done through a subtraction,

$$\begin{aligned} \langle\langle a \rangle\rangle &= \langle\langle a_1 \rangle\rangle - \langle\langle a_3 \rangle\rangle \\ \langle a \rangle &= \langle a_1 \rangle - \langle a_3 \rangle. \end{aligned} \quad (12)$$

### Procedure

We could use the theory described here in several ways to develop an algorithm to attenuate multiples. These different methods go along with the different possible representations of (7). We discuss only one of these methods here, summarized by the following flowchart. We assume that a first-order estimate of the image  $\langle\langle a_1 \rangle\rangle$  from (10) or of  $\langle a_1 \rangle$  from (8) is available. We use also that  $d$ , the field data, are a first order approximation to  $d_1$ , the singly scattered data.



The most difficult portion of this procedure is in the estimation of  $d'$ , and from it  $\mathbf{d}$ . This step also illustrates that if the traveltime monotonicity assumption of ten Kroode is not satisfied, estimating internal multiples requires knowledge of the velocity model to the depth  $z_1$ . Since the location of this layer in the subsurface is not generally known, this means the entire velocity model must be known with enough accuracy to propagate the wavefield through it.

The final step in the algorithm involves differencing two image estimates. In this differencing procedure it is also necessary to compensate for the fact that the contrast at a given position  $(x, z)$  is illuminated differently by multiples than it is by primaries. Thus, even if we were able to estimate the amplitudes of the multiples without error there would still be differences between the multiples estimated from the primary data and the true multiples. Because of this, the subtraction must be done in an adaptive manner such as that suggested by Guitton and Verschuur [2].

Fig. 3(a) illustrates the construction of the third order data,  $\langle d_3 \rangle$ , from three singly scattered data points. In the construction of  $\langle\langle a_3 \rangle\rangle$ , these data contribute to the single scattering isochron with the same source position, receiver position and total traveltime (dashed curve), rather than the three partial time single scattering isochrons (solid curves). The estimate  $\langle\langle a_1 \rangle\rangle$  also puts a contribution from these rays onto the dashed isochron. The subtraction of  $\langle\langle a_3 \rangle\rangle$  from  $\langle\langle a_1 \rangle\rangle$ , removes this incorrect contribution. Also in this plot, a set of rays are shown (dot-dash line) which, due to their identical source-receiver positions and slopes, are difficult to separate in data space. Such kinematically analogous contributions [3] will not pose a problem; the subtraction will result in an amplitude correction.

Figs. 3(b)-(d) illustrate the triple scattering isochron. The three plots together show the set of points which could contribute to a particular point,  $d_3(s, r, t)$ , in the triply scattered data. Each plot shows the contribution from only one of the three scattering points contributing to the multiple, along with the single scattering isochron (dashed-line) corresponding to the time  $t$  illustrated in

## Inverse multiple scattering

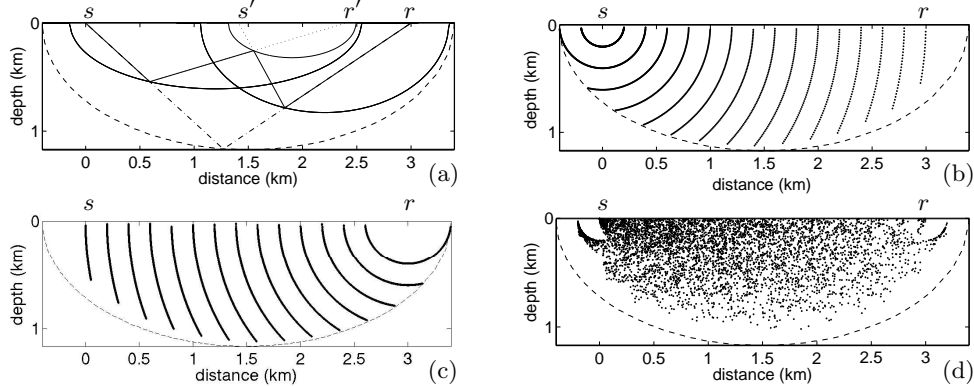


Fig. 3: Isochron construction and triple scattering isochron. In (a), the construction of triply scattered data from singly scattered data is illustrated. The three smaller isochrons are the single scattering isochrons for the three scattering points. The dashed line is the single scattering isochron for the total time  $t$  (illustrated in Fig. 2). Also illustrated in this plot is a contribution indistinguishable from the primary contribution, the rays for which are shown with dot-dashed lines. Plots (b)-(d) show the triple scattering isochron. In (b), only the points from the  $(z_2, s_2, r_2)$  are shown. In (c), only the points from the  $(z_3, s_3, r_3)$  scattering point are shown. In (d), the  $(z_1, s_1, r_1)$  scattering points are shown, although only 1/50 of the number of points in the other plots are shown here. The dashed line is the single scattering isochron for the total traveltime  $t$ .

Fig. 2. The points in (b), which cluster along lines, are from the first scattering point at  $(z_2, s_2, r_2)$ . The points in (c) are from the third scattering point at  $(z_3, s_3, r_3)$ . These two plots are mirror images of one another because of reciprocity (interchanging  $s$  and  $r$  exchanges the first and third scattering points). The spacing between the lines (and between points on them) is governed by the time step used in the computation. In (d), the points from the second scattering point, at  $(z_1, s_1, r_1)$  are shown. These points do not cluster along lines as did those in (b) and (c). The three plots together show that while singly scattered data at a single source, receiver, and time sample the subsurface along an ellipse, triply scattered data at the same source, receiver, and time sample the entire interior of the same ellipse.

### Discussion

We present a theory for the suppression of internal multiples. This theory goes beyond previous theories in that it allows for more general velocity models and is valid in 3D. Our theory, however, relies on knowledge of the velocity model. We suggest suppressing multiples in the image domain rather than the data domain, for two reasons. First, the redundancy in the data makes multiples easier to distinguish in CIGs than in common-shot or common-offset gathers. Second, when estimating multiples in the image domain the multiples need not be modeled to the surface, reducing computation time. Although our method depends on the velocity model, with this dependence we are able to model multiples from all depths and thus remove the requirement of selecting a particular multiple-generating horizon in the data before processing. Even if this horizon is known, with our method computing the multiples generated from a region surrounding this horizon is straightforward. Doing this will reduce errors in the estimated multiples caused by errors in picking the horizon.

### References

- [1] M. V. de Hoop. Generalization of the Bremmer coupling series. *J. Math. Phys.*, 37:3246–3282, 1996.
- [2] A. Guitton and D. J. Verschuur. Adaptive subtraction of multiples using the  $L_1$ -norm. *Geoph. Prosp.*, 52:27–38, 2004.
- [3] F. Hron. Numerical methods of ray generation in multilayered media. *Methods in computational physics*, 12:1–34, 1972.
- [4] P. Sava and A. Guitton. Multiple attenuation in the image space. *submitted, Geophysics*, 2004.
- [5] C. C. Stolk and M. V. de Hoop. Modeling of seismic data in the downward continuation approach. *submitted to SIAM J. Appl. Math.*, 2004. CWP468P.
- [6] C. C. Stolk and M. V. de Hoop. Seismic inverse scattering in the downward continuation approach. *submitted to SIAM J. Appl. Math.*, 2004. CWP469P.
- [7] A. P. E. ten Kroode. Prediction of internal multiples. *Wave Motion*, 35:315–338, 2002.
- [8] A. Weglein, F. A. Gasparotto, P. M. Carcalho, and R. H. Stolt. An inverse-scattering series method for attenuating multiples in seismic reflection data. *Geophysics*, 62:1975–1989, 1997.

### Acknowledgments

This work was supported by the sponsors of the Consortium Project on Seismic Inverse Methods for Complex Structures at the Center for Wave Phenomena and by Total.